

## Multiparametric microvascular MRI: a cluster approach to characterize glioma

Nicolas Coquery<sup>1,2</sup>, Clément Debacker<sup>3,4</sup>, Régine Farion<sup>2,5</sup>, Chantal Rémy<sup>1,2</sup>, Olivier Francois<sup>6,7</sup>, and Emmanuel Luc Barbier<sup>1,2</sup>

<sup>1</sup>U836, INSERM, Grenoble, France, <sup>2</sup>Université Joseph Fourier, Grenoble, France, <sup>3</sup>Université Joseph Fourier, Grenoble, France, <sup>4</sup>Brüker Biospin MRI, Ettlingen, Germany, <sup>5</sup>Grenoble MRI Facility IRMaGe, Grenoble, France, <sup>6</sup>TIMC-IMAG laboratory, UMR5525, CNRS, La Tronche, France, <sup>7</sup>Université Joseph Fourier, La Tronche, France

### Introduction

It is well-known that tumor growth impacts the microvasculature. Several microvascular characteristics can be mapped with MRI: apparent diffusion constant (ADC), cerebral blood volume (CBV) [1] and flow (CBF), integrity of the vascular wall assessed by the area under curve after Gd-DOTA injection ( $AUC_{Gd-DOTA}$ ) [2], tissue oxygen saturation ( $StO_2$ ) [3], and cerebral metabolic rate of oxygen ( $CMRO_2$ ). This accumulation of information is not readily interpretable. However, there are tight physiological links between these microvascular features. For example, a reduction in CBV should impact CBF and  $StO_2$ . It might thus be possible to define clusters of pixels with similar microvascular characteristics. In this study, two orthotopic glioma models were characterized with microvascular MRI. Data were analyzed using a model-based cluster approach.

### Materials and methods

The C6 model (Wistar rats,  $n=13$ ) was inoculated with  $10^5$  cells in 5  $\mu$ L and the F98 model (Fischer rats,  $n=13$ ) was inoculated with  $10^3$  cells in 5  $\mu$ L. Microvascular MRI was performed at 4.7 T (Avance III; Bruker) between 22 and 26 days after tumor inoculation. Six MRI parameters were mapped: ADC (TR/TE = 3000/28.6 ms,  $b=0$  and 900  $s/mm^2$ ), vascular wall integrity assessed with a DCE-MRI approach and the calculation of the AUC following an intravenous injection of a Gd-chelate [2], CBF using continuous arterial spin labeling (ASL; spin-echo EPI, TE=17.2ms, labeling duration=4s, postlabeling delay=0.2s, 20 pairs), CBV and  $StO_2$  as previously described [3]. A  $CMRO_2$  map was computed using  $CMRO_2 = CBF \times (1 - StO_2/100)$ .

A model-based cluster analysis was performed on voxels obtained from the 26 animals (13 animals/model) in three regions of interest (ROI; total voxels number=3405) manually drawn on the  $T_2$ -weighted ( $T_2w$ ) image with the largest tumor surface: *tumor* ( $n=2525$  voxels), *contralateral striatum* ( $n=347$  voxels) and *cortex* ( $n=533$  voxels). Normal mixture modeling was performed on voxel data using Expectation-Maximization algorithms implemented in the R package mclust [4]. Model choice and the optimal number of clusters ( $k=5$  clusters) were determined with a Bayesian information criterion [4].

### Results/Discussion

A qualitative look on the MRI maps suggests that the decrease in CBF,  $StO_2$  and  $CMRO_2$  is more pronounced in the F98 than in the C6 glioma (Fig.1A). The model-based cluster analysis (Fig.2B-C) of 5 clusters shows that the contralateral cortex and striatum are mainly composed of the same cluster (red), which can thus be related to "healthy" voxels. The four other clusters (orange, yellow, blue, and purple) are found in tumors. The orange cluster is similar to the red cluster but has higher CBV and ADC. This cluster also appears in healthy tissue. The yellow cluster corresponds to a reduction in CBV and a surprising increase in  $CMRO_2$ . The blue cluster has reduced CBV and increased ADC. The purple cluster shows more pronounced decreases in CBF,  $StO_2$  and  $CMRO_2$  and more pronounced increases in AUC and ADC. The two tumor models have different cluster compositions (Fig.1D): the C6 model is heterogeneously composed of all clusters, whereas the F98 model is mainly composed of the purple cluster, in agreement with our qualitative observations (Fig. 1A). In both cases, the cluster-based analysis preserves a spatial organization within the tumor.

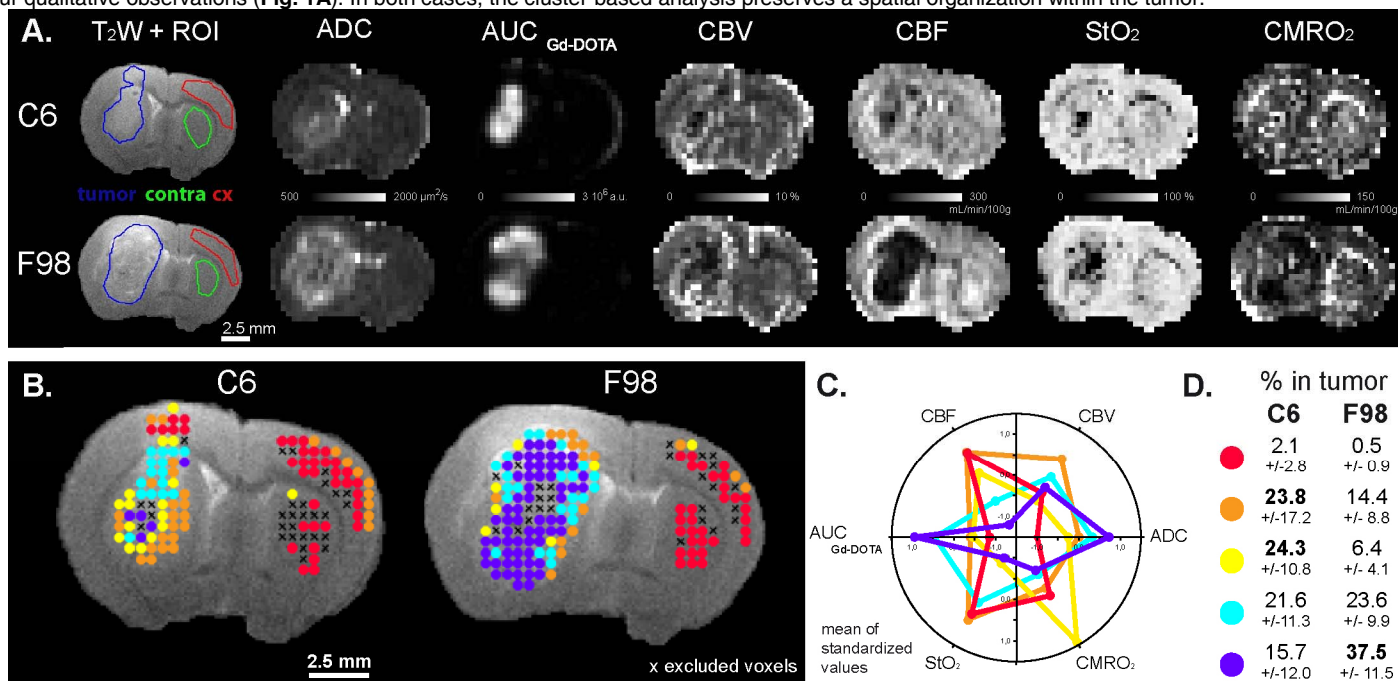


**Figure 1:** (A)  $T_2w$  images from C6 and F98 glioma models. ROI are depicted: tumor (blue), contralateral striatum (green) and cortex (red). Parameter maps: ADC,  $AUC_{Gd-DOTA}$ , CBV, CBF,  $StO_2$ ,  $CMRO_2$ . (B) Distribution of the five clusters in each ROI. Color code is related to (C) where all parameters are described as the mean of standardized values for each cluster. (D) Mean±Standard Deviation fraction of the each cluster in the two tumor models. Black crosses represent excluded voxel with non-physiological values at least in one MRI parameter (m+/-sd fraction in tumor: C6: 12.5+/-11.5 and F98: 17.7+/-10.0).

### Conclusion

Cluster analysis can be used to structure the wealth of information gathered with multiparametric microvascular MRI. The cluster-based analysis highlights several types of physiological behavior, which could correspond to different levels of the tumor evolution. A cluster-based analysis of the tumor microvascular characteristic has a great potential to ease tumor diagnosis, prognosis, and treatment follow-up and detect tumor areas that could become resistant to treatment.

**References:** [1] Valable et al., *NMR Biomed*, 21, 1043-1056, 2008; [2] Lemasson et al., *Radiology*, 257, 342-352, 2010 ; [3] Lemasson et al., *Radiology*, epub, 2012 ; [4] Fraley and Raftery, *Journal of the American Statistical Association*, 97, 611-631, 2002.